

## Petrophysical Evaluation by Integrating AI and HFU Methods. A Case Study of the Mishrif Reservoir in Southern Iraq

Layth H. Abd Ali  \*, Sameera M. Hamd-Allah  

Department of Petroleum Engineering, College of Engineering, University of Baghdad, Baghdad, Iraq

### ABSTRACT

**R**eservoir quality assessment is important for detecting hydrocarbon-bearing zones and guiding future enhancement strategies. This study presents a detailed petrophysical evaluation of the Mishrif Formation in the Buzurgan Oilfield, which was selected due to its strategic value through its significant remaining reserves which making it an ideal candidate for advanced evaluation techniques. This study aims for shale content, porosity, permeability, water saturation, net to gross, and lithology determination. Well log and core data were used together to establish accurate property estimations. Permeability prediction through conventional methods, like core permeability-porosity correlations, was highly dispersive due to the heterogeneity of the carbonate formation. To ensure accurate permeability prediction, the Hydraulic Flow Unit method was employed with the Bootstrap Forest-AI model. The research results reveal that MB21 is the principal pay zone, which exhibits high porosity, low water saturation (high hydrocarbon saturation), and low shale content. These zone favorable properties make it encouraging for future development through drilling more production wells in this zone. This study presents a novel hybrid approach that integrates classical petrophysical approaches with an AI model, providing a robust platform for reservoir characterization.

**Keywords:** Reservoir characterization, Artificial intelligence, Bootstrap forest method, Hydraulic flow unit, Buzurgan oilfield.

### 1. INTRODUCTION

Accurate evaluation of petrophysical properties is essential for every operation in the hydrocarbon industry. (Shah et al., 2021). Petrophysical evaluation systematically analyzes the properties of subsurface rock and fluids using well logs and core measurements. It analyzes various well logs as gamma-ray, density, neutron, sonic, and resistivity logs, to determine reservoir characteristics, including porosity, permeability, fluid saturation, lithology, and Net-To-Gross.(Bateman, 2012; Zelenika et al., 2017).

\*Corresponding author

Peer review under the responsibility of University of Baghdad.

<https://doi.org/10.31026/j.eng.2025.09.11>



This is an open access article under the CC BY 4 license (<http://creativecommons.org/licenses/by/4.0/>).

Article received: 16/03/2025

Article revised: 28/04/2025

Article accepted: 06/05/2025

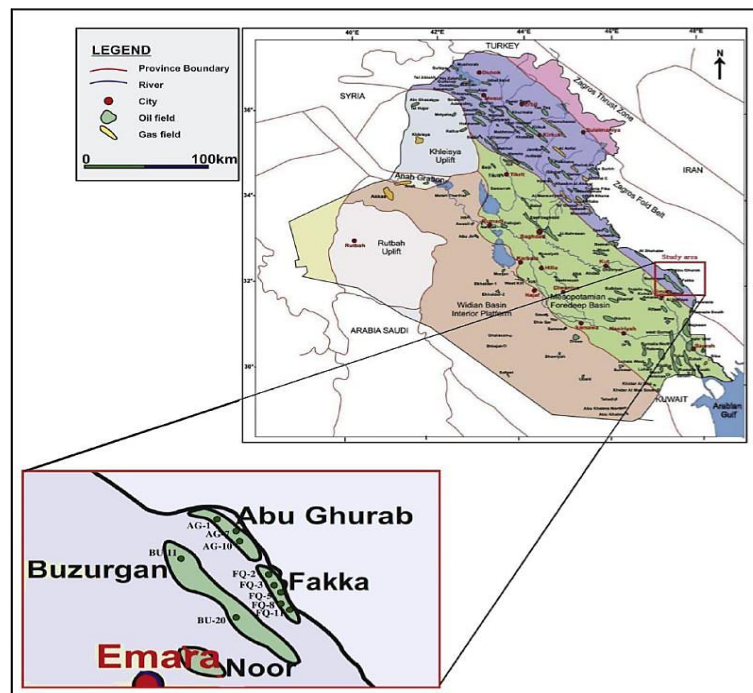
Article published: 01/09/2025

Permeability is a crucial petrophysical property that controls fluid flow through a reservoir. (Al-Dujaili et al., 2021). There are various methods to estimate permeability, such as core analysis, which represents the most reliable approach. However, due to the limited core tests, well-log-based techniques are used indirectly. One of the most effective techniques for predicting permeability in heterogeneous reservoirs is the Hydraulic Flow Unit (HFU) method, which categorizes rock units based on their flow behavior and petrophysical characteristics. (Amaefule et al., 1993; Tiab and Donaldson, 2012; Anifowose et al., 2013; Al-Ameri and Hamd-Allah, 2023; Abdulelah et al., 2018; Al-Dujaili, 2023). Machine learning algorithms such as Artificial Neural Networks (ANNs), Support Vector Machines (SVMs), and Decision Tree Algorithms can mimic complex, non-linear relationships between petrophysical properties and permeability accurately. (Abd Ali and Hamd-Allah, 2026; Abnavi et al., 2021; Al Hussein and Hamd-Allah, 2024).

This research presents the petrophysical evaluation of five wells within the Mishrif reservoir in Buzurgan Oilfield. The formation lithology, shale volume, porosity, saturation, and NTG are established. Furthermore, permeability prediction by using the HFU method based on an AI model was developed.


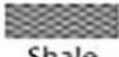





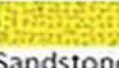

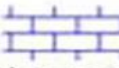

## 2. GEOLOGICAL SETTING

The Buzurgan oilfield is located southeastern part of Iraq near the Iran boundary. Discovered in 1970, its development began in 1976 (Khashman et al., 2025). Structurally, it is characterized by an asymmetrical anticline that extends from NW to SE direction, with two domes that are separated by a structural saddle. (Aldarraji and Almayahi, 2019; Mohammed and Salih, 2025) As shown in Fig. 1, the Mishrif formation is divided into 7 zones, namely MA, MB11, MB12, MB21, MB22, MC1, and MC2. MA consists mainly of compact limestone with some packstone reservoirs. MB11 consists mainly of mudstone interbedded with thin wackestone reservoirs.



**Figure 1.** The Iraq map shows the Buzurgan oilfield's location and direction (Alhusseini and Hamd-Allah, 2022).

MB12 consists of mudstone. MB21 is mainly composed of grainstone and packstone. One. MC1 is mainly composed of a packstone reservoir in the upper part and compact mudstone in the lower part. MC2 mainly consists of packstone. The geological column of the field is demonstrated in **Fig. 2 (Ahmed, 2022)**.

Age	Formation	Lithology	Description	Symbol
Neocene	Bachitary, upper, Medium, and Lower Fars		Represent by Clay, Shale, anhydrite, some sandstone, Clay shale and White Dolomite	 Shale
				 Clay
Lower Miocene to Oligocene	Asmari		Limestone, Dolomite and Anhydrite, and Dolomitic shale	 Anhydrite
				 Sandstone
Cretaceous			Clay, limestone, Clay shale, Sandstone, and Dolomite	 Limestone
Turonian to upper Cenomanian	Mishrif		Mainly Limestone and characterized by thin layer on the top, limestone vary from soft to medium and hard (Mudstone, Packstone, Wackstone, Grainstone )	

**Figure 2.** Stratigraphy column and description of the field (Ahmed, 2022).

### 3. MATERIALS AND METHODS

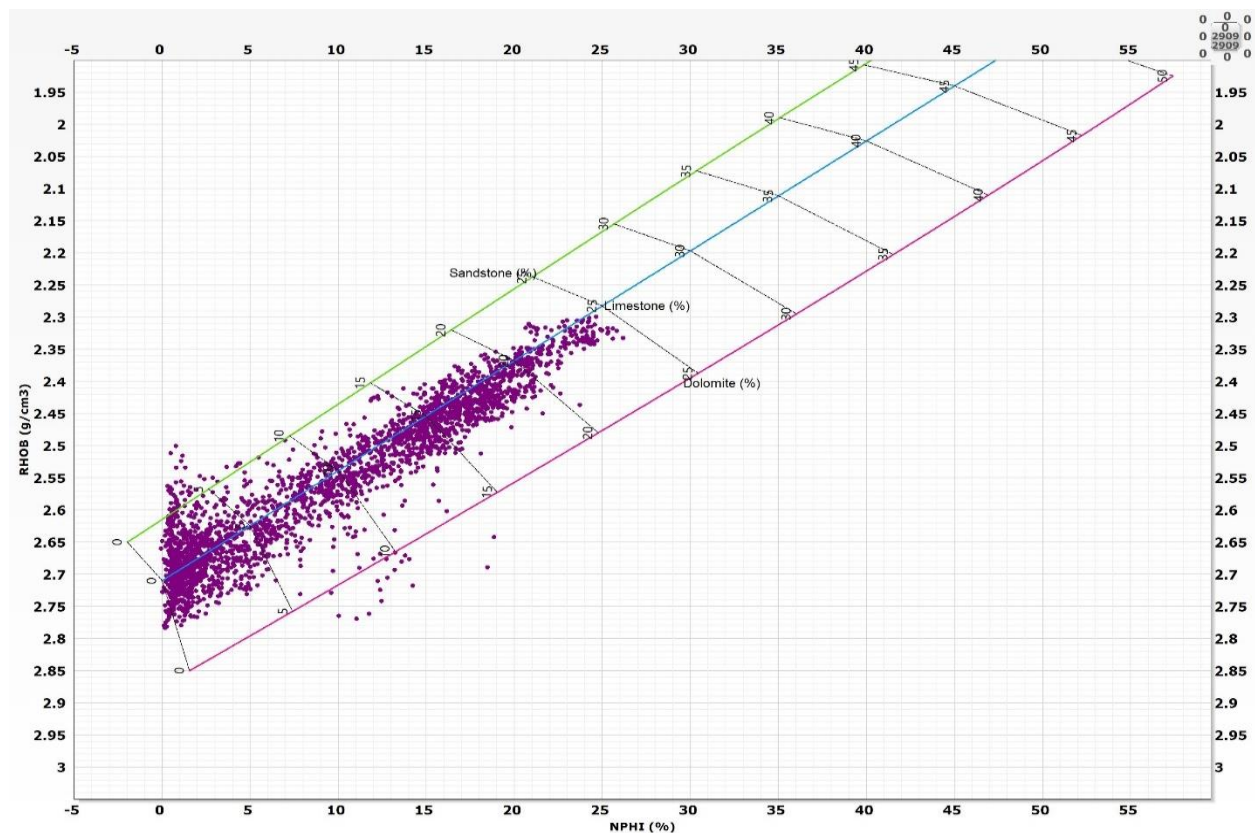
This research presents a comprehensive petrophysical evaluation of five wells (Y1, Y2, Y3, Y4, and Y5) within the Mishrif reservoir in the Buzurgan oilfield. Well log data (gamma-ray, sonic, neutron, density, and resistivity logs) in conjunction with available core measurements of permeability and porosity were utilized to achieve the study's Purpose.

Additionally, wellhead and well-top data were incorporated to enhance the stratigraphic and structural analysis. Advanced techniques such as Hydraulic Flow Units and Artificial Intelligence methods were applied to improve the accuracy of petrophysical properties determination by using petroleum and statistics software. The most difficult step in the HFU method is determining the Flow Zone Indicator in the unsampled wells. To overcome this obstacle, the Bootstrap Forest model was used to predict the value of FZI using well logs only.

## 4. RESULTS AND DISCUSSION

### 4.1 Lithology Determination

Accurate lithology identification is a critical step in reservoir characterization because it directly influences subsequent calculations of porosity, water saturation, and permeability. A proper understanding of lithology ensures the validity of petrophysical interpretation, enhances the quality of reservoir modeling, and increases the prediction of hydrocarbon-bearing zones. The Density Neutron cross plot is among the most widely applied techniques used for lithology identification and provides an effective technique for rock-type separation based on petrophysical response. (Dewan, 1983; Rider, 2002; Sebtosheikh et al., 2015). The cross plot can distinguish between sandstone, limestone, and dolomite lithologies through the comparison of the neutron and density log response and enable geoscientists and engineers to assess reservoir quality and heterogeneity with greater confidence. **Fig. 3** illustrates the lithology of the reservoir, confirming that the dominant rock type is limestone.



**Figure 3.** Density Neutron cross plot for lithology identification.





## 4.2 Shale Volume Calculation

Shale existence in the formation has a major effect on all principles of reservoir characteristics, including reduced permeability and effective porosity, which leads to uncertainties in formation evaluation and the appropriate estimation of oil and gas reserves. (Bassiouni, 1994; Causey, 1991). In the current work, shale volume is estimated from the gamma-ray. The initial step involves calculating the gamma-ray index ( $I_{GR}$ ) using the following equation:

$$I_{GR} = \frac{GR_{log} - GR_{min}}{GR_{max} - GR_{min}} \quad (1)$$

Where GRlog: the gamma ray reading of formation, GRmin: the minimum gamma ray (clean carbonate), and GRmax: the maximum gamma ray (shale). For older rocks, such as the Cretaceous formations in the Buzurgan oilfield, the Larionov equation was applied to calculate Shale volume.  $V_{sh}$  :

$$V_{sh} = 0.33(2^{2 \cdot I_{GR}} - 1) \quad (2)$$

The result of shale volume calculations is shown in Fig. 4.

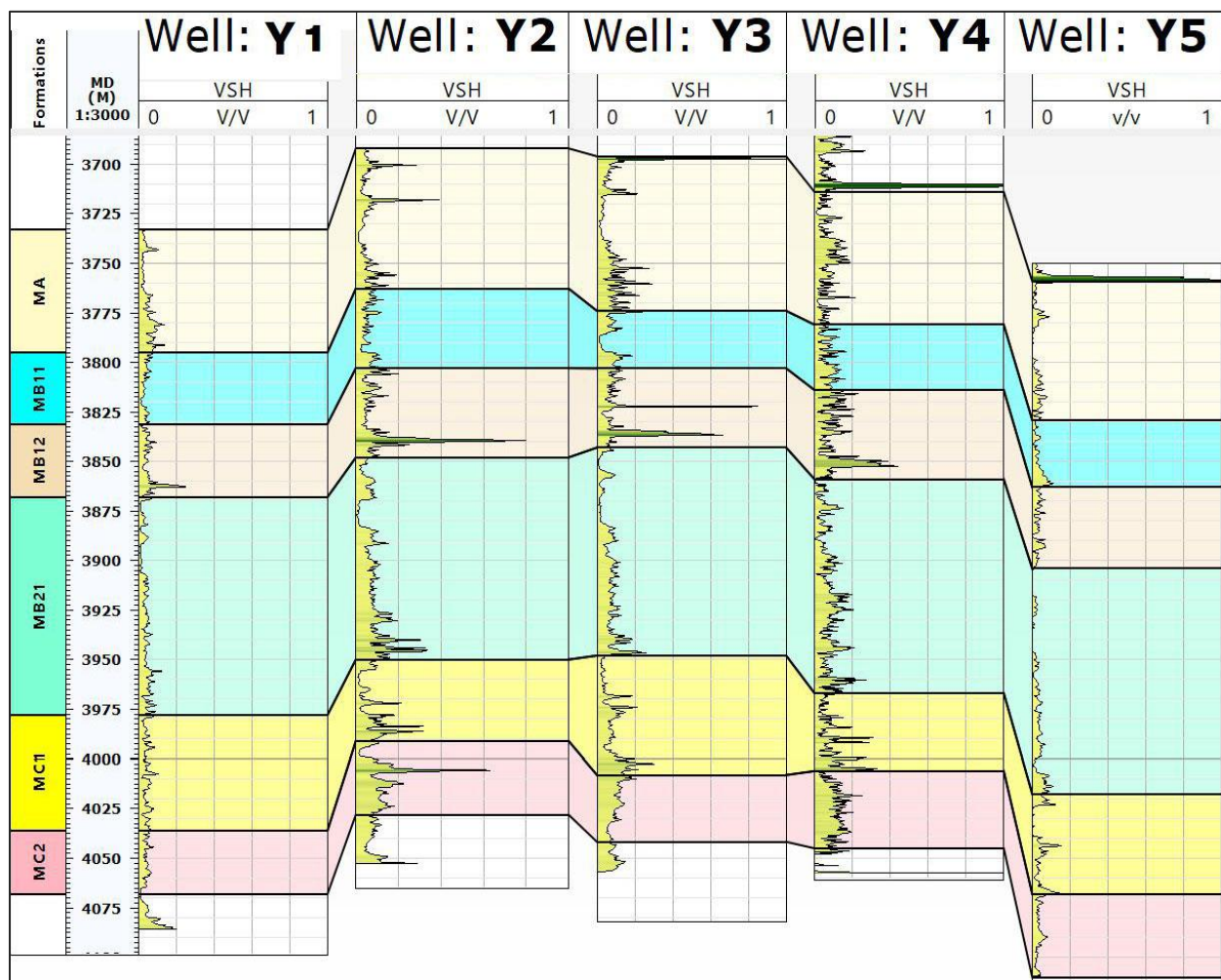


Figure 4. Shale content results.



### 4.3 Porosity Determination

The total porosity log is calculated from density, sonic, and neutron-density log records. (Horsfall et al., 2013; Schön, 2011).

$$\phi_D = \frac{\rho_{ma} - \rho_b}{\rho_{ma} - \rho_f} \quad (3)$$

$$\phi_s = \frac{\Delta t_{log} - \Delta t_{ma}}{\Delta t_f - \Delta t_{ma}} \quad (4)$$

$$\phi_{ND} = \frac{\phi_D + \phi_N}{2} \quad (5)$$

Where:  $\phi_D, \phi_s, \phi_{ND}$ : are the density, sonic, and neutron-density derived porosities, fraction.

$\rho_{ma}$ : is the matrix density, 2.71 gm/cc for limestone.

$\rho_b$ : is the formation bulk density, gm/cc.

$\rho_f$ : is the fluid density, 1 gm/cc for fresh water or 1.1gm/cc for salt water.

$\Delta t_{ma}$ : is the interval transit time in the matrix, 47.6  $\mu$ sec/ft for Limestone.

$\Delta t_{log}$ : is the interval transit time in the formation,  $\mu$ sec/ft; and

$\Delta t_f$ : is the interval transit time in the fluid within the formation, 189 or 185  $\mu$ sec/ft for fresh water and salt-water mud, respectively.

The calculated porosities are validated with available core porosity and found that the accurate porosity log composited from most of the methods depending on the situation as shown in the last track in **Fig. 5**. For example, sonic porosity is taken in the caved intervals, the density porosity is taken in the shale intervals, and the neutron-density porosity is taken for the non-problematic intervals, as shown in **Fig. 5**.

The determined total porosity log (POR) best matches the porosity from the core, as shown in the following **Fig. 5**. So, we can rely on this method of interpretation for other uncored wells. The effective porosity (PHIE) represents our target in this step and was calculated from the following equation. (Stephens et al., 1998):

$$PHIE = POR - \phi_{sh} * V_{sh} \quad (6)$$

Where ( $\phi_{sh}$ ) represents the porosity of the clay (shale). **Fig. 6** presents the determined effective porosity log of the five wells.

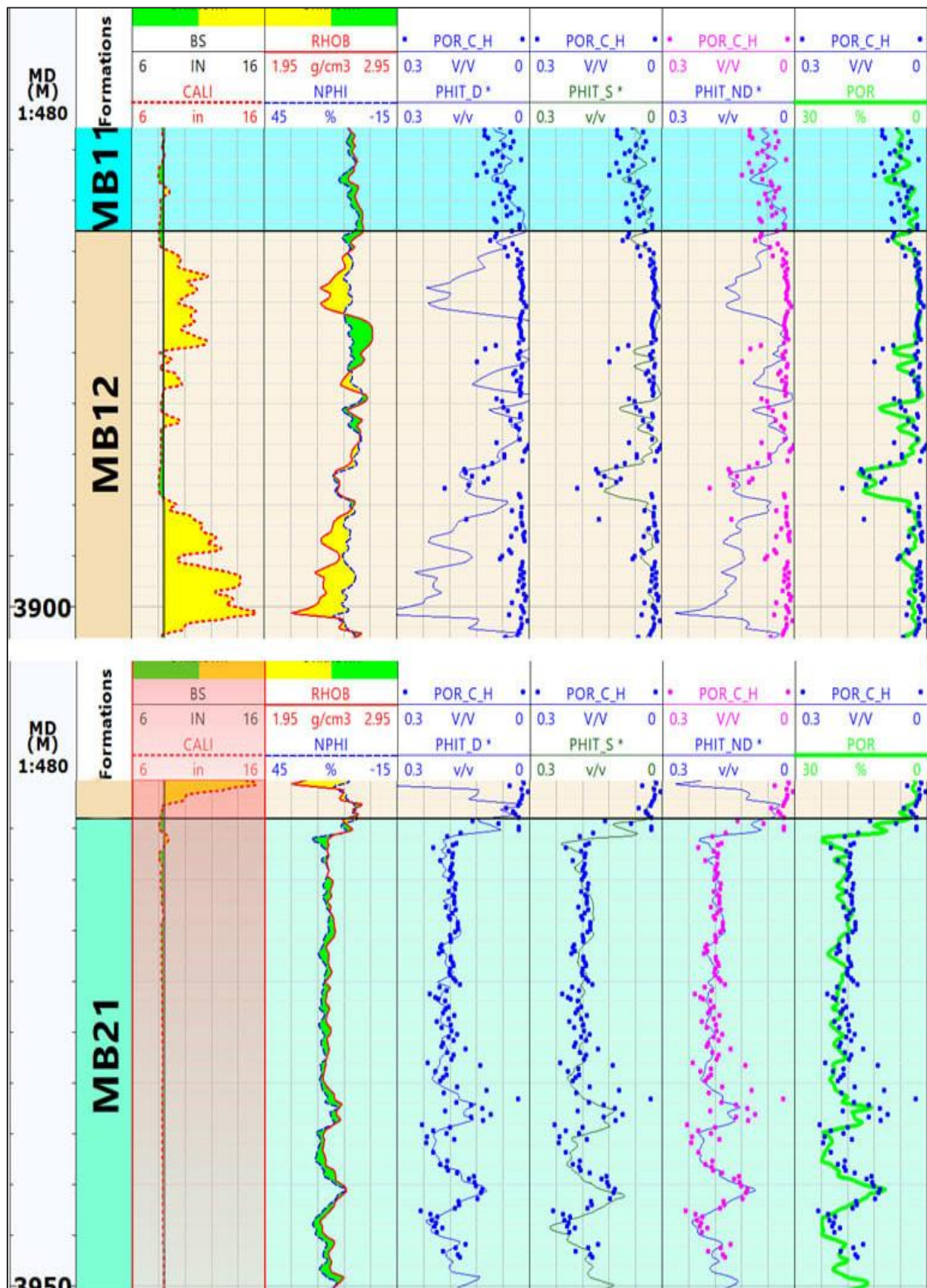
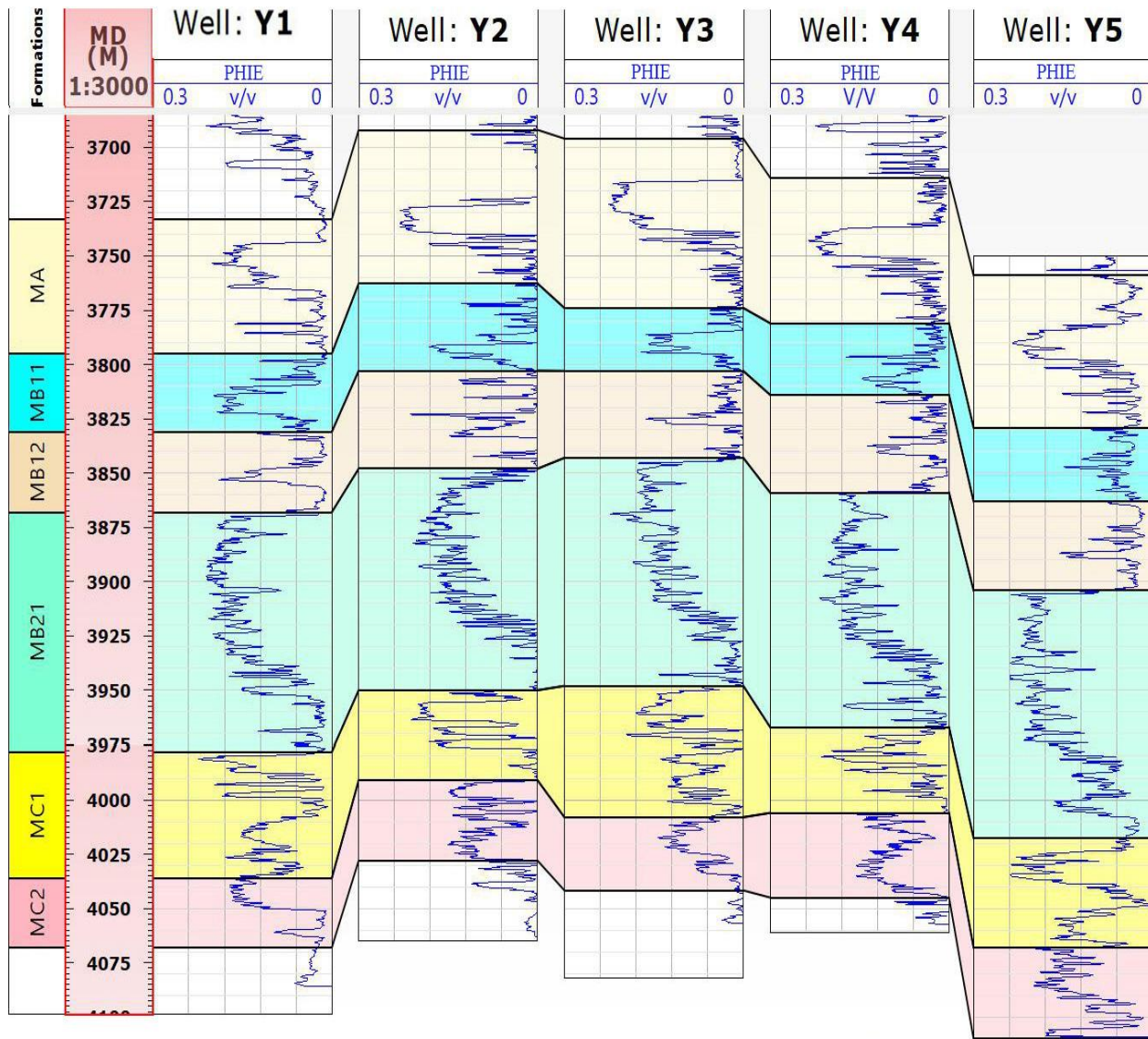


Figure 5. Total Calculated porosity with core porosity.





**Figure 6.** Effective porosity for the five wells.

#### 4.4 Water Saturation Calculations

The Archie equation formula is used for calculating water saturation:

$$S_w = \left( \frac{a \times R_w}{R_T \times PHIE^m} \right)^{(1/n)} \quad (7)$$

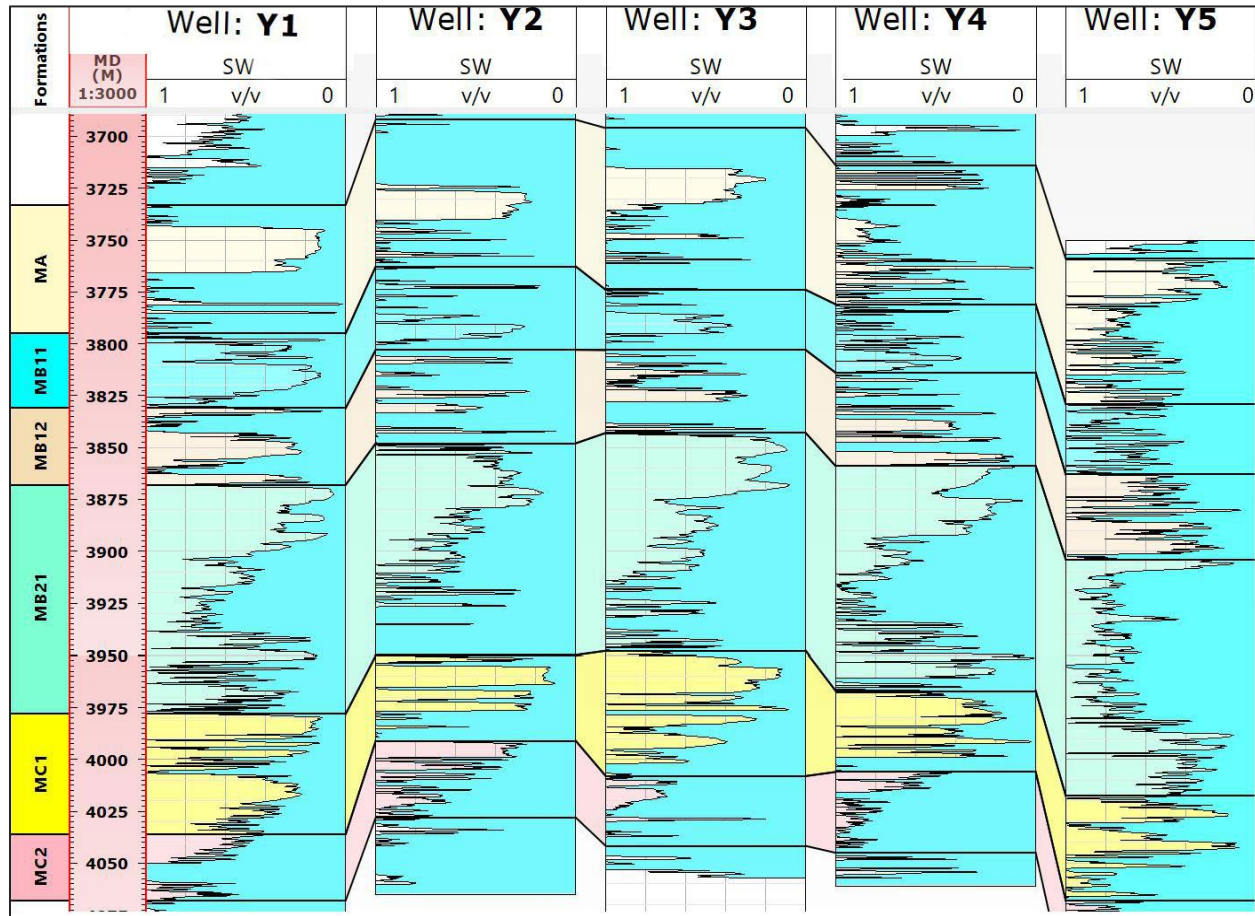
Where PHIE-effective porosity,  $R_T$ -formation resistivity, and  $R_w$ - formation water resistivity. It is preferred to identify  $a$ , which is a constant depending on lithology,  $m$ -cementation exponent, associated with the pore structure,  $n$ -saturation exponent, associated with rock wettability, by the special core analysis. (Al-Dujaili et al., 2023). Still, due to a lack of this report, the values were taken as 1, 2, and 2, respectively. (Worthington, 1993; Pickett, 1966).

Some parameters may be changed according to the actual situation, such as  $R_w$ , as in Table 1, and Fig. 7 shows the calculated water saturation.



**Table 1.** Water resistivity parameter for the wells.

WELL	Y1	Y2	Y3	Y4	Y5
Rw	0.018	0.025	0.018	0.02	0.02

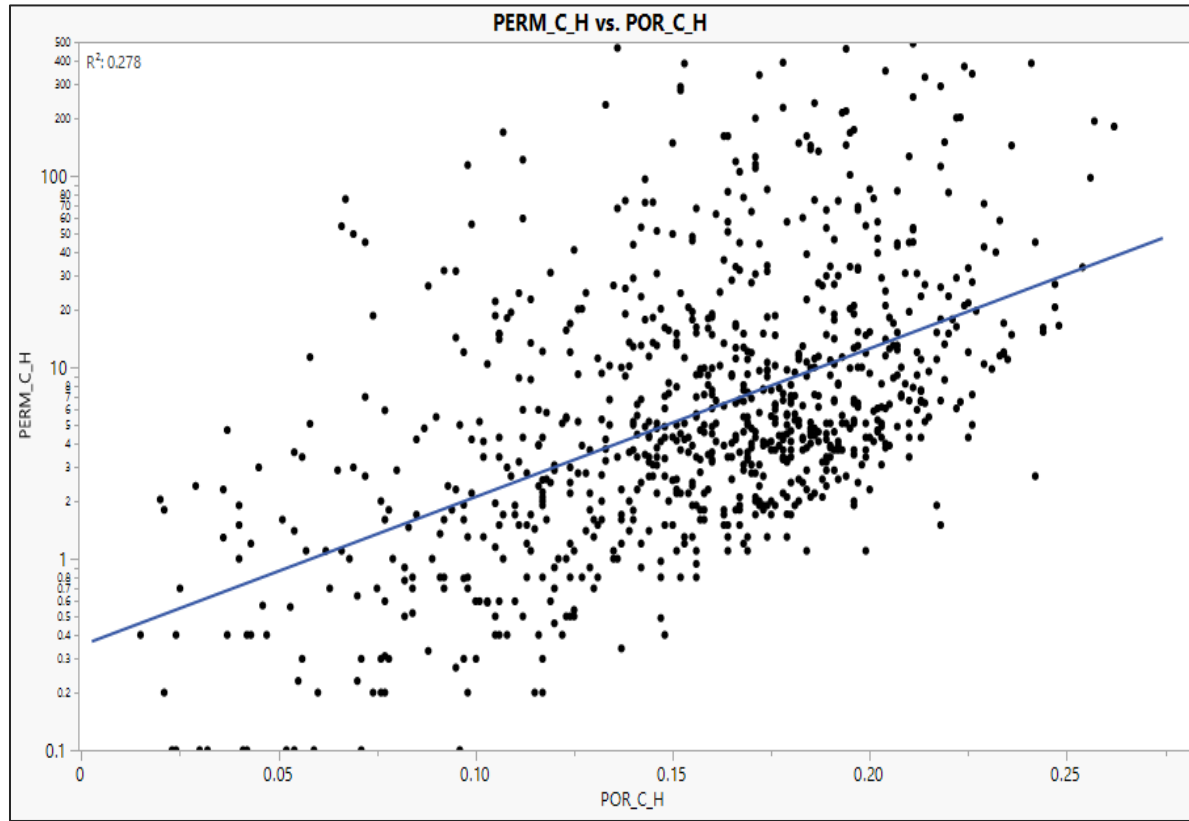
**Figure 7.** Water saturation calculation.

#### 4.5 Permeability Estimation

Permeability is a crucial reservoir rock property due to the hydrocarbon production rate is mainly dependent on its value. The most reliable local permeability values may be obtained from core analysis. As a result of limitations of core data availability, the permeability values in most wells along the reservoir are usually evaluated from other indirect methods. (Zhang et al., 2019; Mohammadian et al., 2022; Skrettingland et al., 2011; Abd Ali and Hamd-Allah, 2026; Alobaidi, 2016).

##### 4.5.1 Permeability Estimation from Classical Method

Permeability estimation through the relationship between permeability and porosity core in the Mishrif carbonate reservoir shows significant dispersion in the relationship, reflected by a low R<sup>2</sup> of 0.278, which highlights the formation of heterogeneity as shown in Fig. 8. Therefore, porosity alone is insufficient to accurately analyze and predict the permeability.



**Figure 8.** Core porosity against core permeability.

#### 4.5.2 Permeability Estimation Using the HFU Method Enhanced by Bootstrap Forest

In this part of the research paper, the Artificial Intelligence (AI) technique called Bootstrap Forest (BF) is employed with the Hydraulic Flow Unit (HFU) method to improve the permeability estimation accuracy. HFU method incorporates the reservoir quality index (RQI) and normalized porosity ( $\phi_z$ ) for Flow Zone Indicator (FZI) calculation in cored wells through the following equations (Amaefule et al., 1993; Hamd-Allah et al., 2016; Anifowose et al., 2013; Astsauri et al., 2024; Borhani and Emadi, 2011).

$$RQI = 0.0314 \sqrt{\frac{k}{\phi_e}} \quad (8)$$

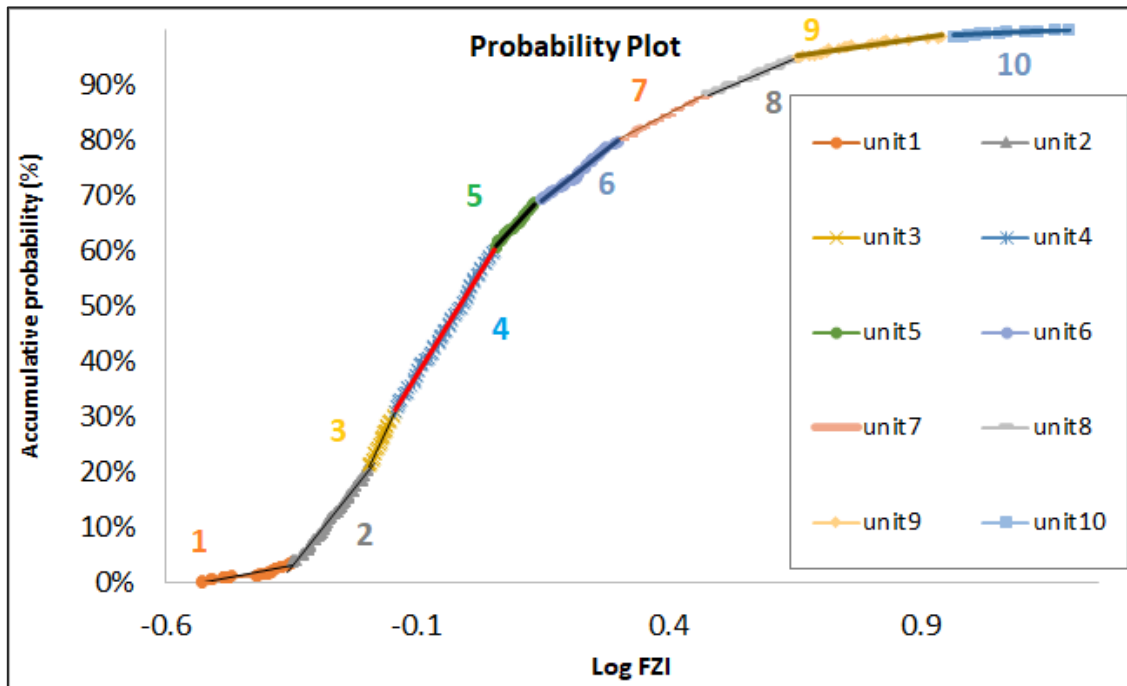
$$\phi_z = \frac{\phi_e}{1 - \phi_e} \quad (9)$$

$$FZI = \frac{RQI}{\phi_z} \quad (10)$$

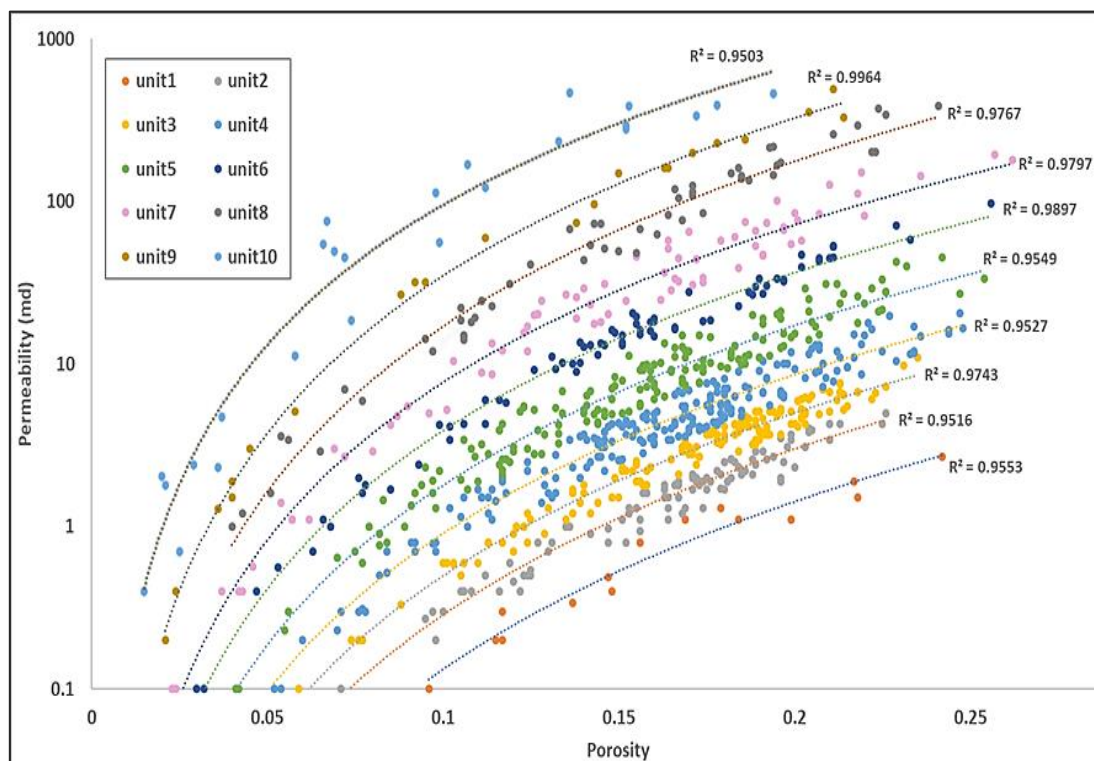
By using a probability plot to identify the number of HFUs of the Mishrif formations. **Fig. 9** shows ten lines that suggest the presence of ten HFUs in the Mishrif Formation. This classification improved the porosity-permeability relationship. (Al-Rikaby and Al-Jawad, 2024) As demonstrated in **Fig. 10** and **Table 2**.

The Bootstrap Forest model is used to predict the value of the Flow Zone Indicator (FZI) using well logs to use in permeability estimation through the flowing equation.

$$K = 1014 * FZI^2 * \frac{\phi_e^3}{(1 - \phi_e)^2} \quad (11)$$



**Figure 9.** Probability plot of Logarithm FZI.



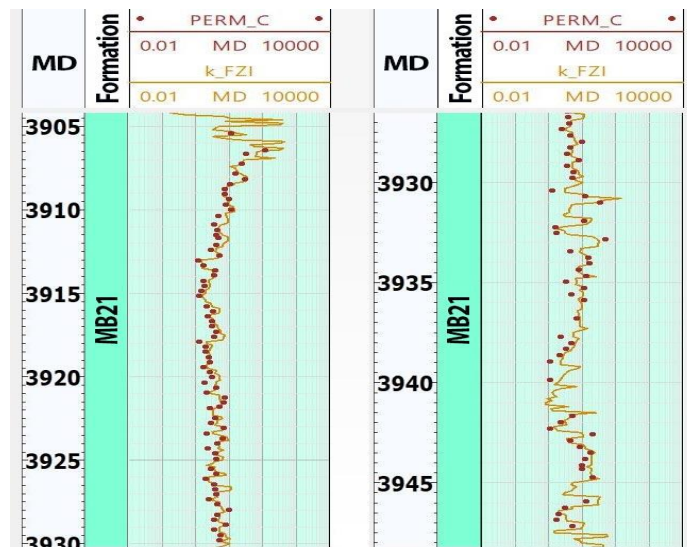
**Figure 10.** Permeability core vs. porosity core for the HFUs.

**Fig. 11** indicates excellent agreement of the permeability calculated with the core permeability measurement for a well in the study case. This validation confirms the validity of the estimation method utilized, which provides confidence in the reliability of the permeability predictions. Thus, the final permeability is presented in **Fig. 12**.



**Table 2.** Hydraulic Flow Units parameters.

HFU NO.	Permeability Prediction Eq.	R <sup>2</sup>	HFU Color
1	$k=355\Phi^{3.428}$	0.955	Orange
2	$k=703\Phi^{3.39}$	0.952	Grey
3	$k=1064\Phi^{3.33}$	0.974	Yellow
4	$k=1599\Phi^{3.25}$	0.953	Light Blue
5	$k=3298.9\Phi^{3.26}$	0.955	Green
6	$k=664.3\Phi^{3.23}$	0.989	Dark Blue
7	$k=1280\Phi^{3.22}$	0.979	Pink
8	$k=405\Phi^{3.38}$	0.977	Dark Grey
9	$k=583\Phi^{3.22}$	0.996	Orange
10	$k=6862\Phi^{2.86}$	0.95	Blue

**Figure 11.** Predicted permeability and core permeability profile.

#### 4.6 NTG

The volumetric computations of initial hydrocarbon in place require the net-to-gross thickness, which is an essential parameter in petroleum reservoir engineering. Generally, the cut-off parameters are utilized to detect the reservoir quality and the productive zones. (Al Jawad and Tariq, 2019; Bouffin and Jensen, 2009; Egbele et al., 2005). In the current work, Techlog software 2015 is used to compute net to gross thickness for wells. The main input data were log results for porosity and water saturation, as well as the shale volume, and their cut-off values. Fig. 13 shows NTG calculations.

The results presented in the mentioned figures indicate that the primary pay zone across all five wells is the MB21 unit, which exhibits a high porosity, low water saturation, and low shale content. This unit is characterized by high reservoir quality, making it the dominant contributor to hydrocarbon production. For MC1, the net-to-gross (NTG) ratio is lower than MB21 due to the fact that it contains comparatively lesser porosity and moderate water saturation. MC2, however, contains a very high water saturation as it occurs closer to the oil-water contact (OWC) and is therefore not a good hydrocarbon-bearing interval. While the MA, MB11, and MB12 units exhibit poor petrophysical properties with low porosity, high shale volume, and low hydrocarbon saturation, hence less productive.

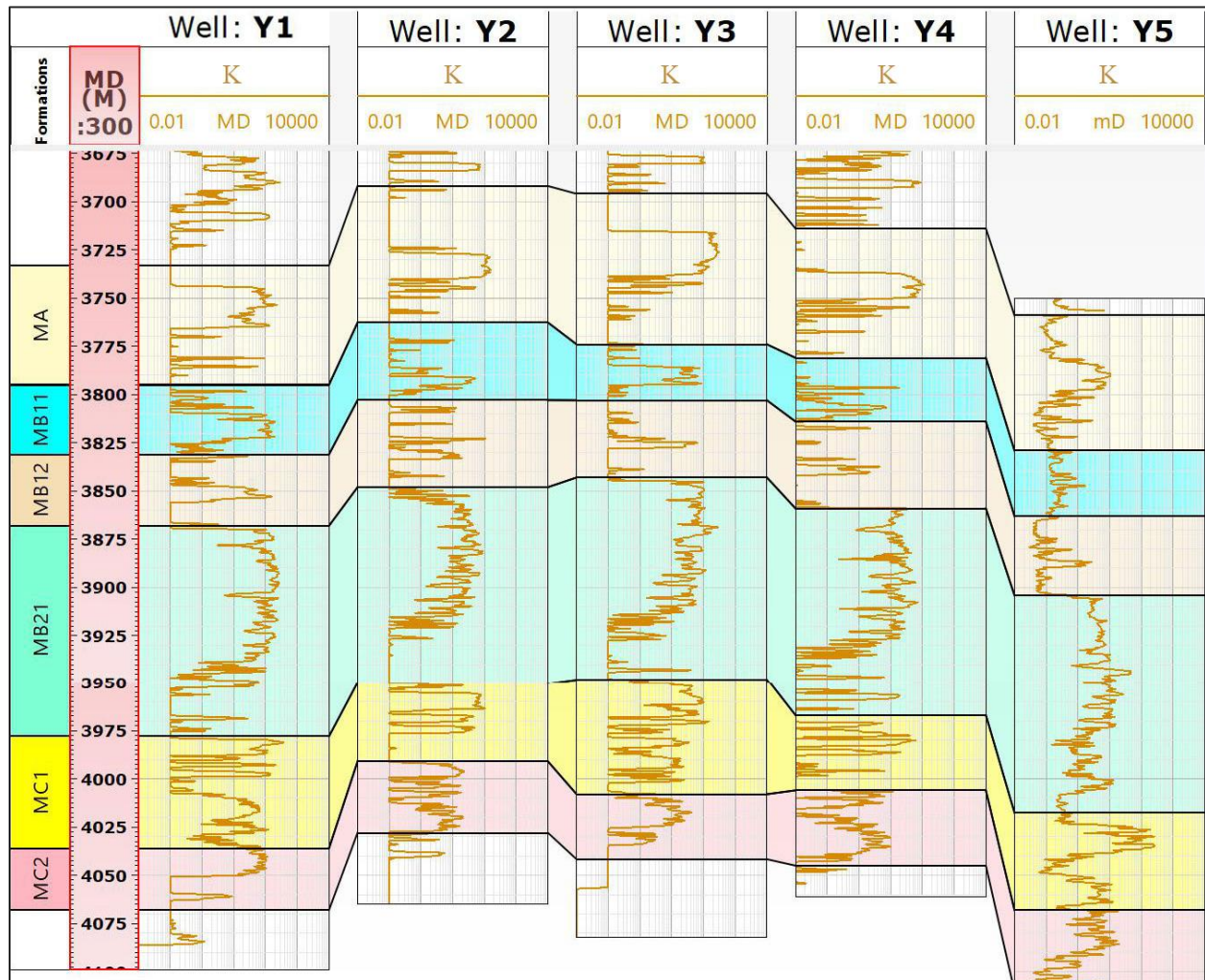


Figure 12. Wells predicted Permeability.



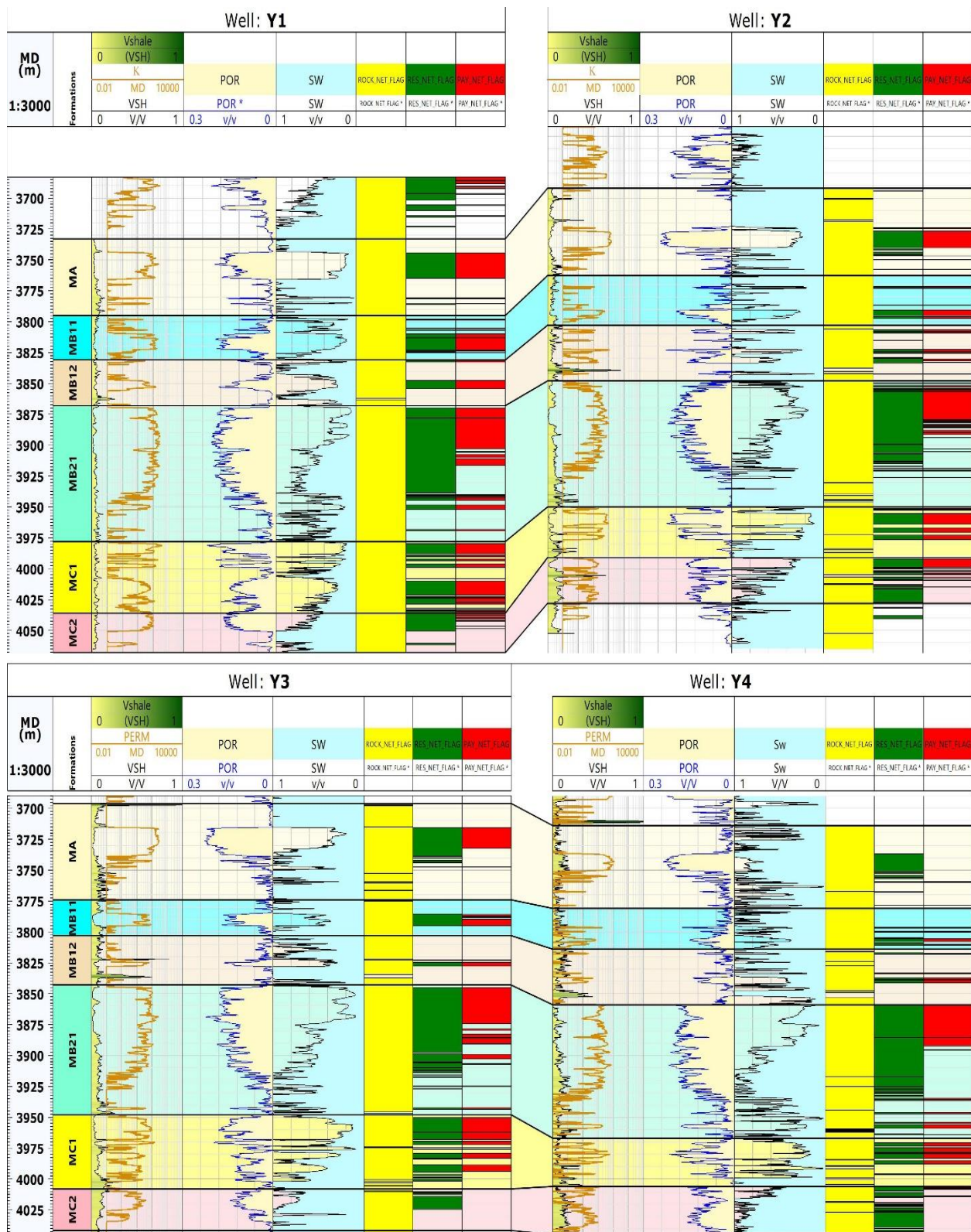


Figure 13. Net to gross of wells Y1, Y2, Y3, and Y4.





## 5. CONCLUSIONS

This study provides an integrated petrophysical analysis of the Mishrif Formation in the Buzugan Oilfield and showing the success of integrating Artificial Intelligence (AI) with conventional petrophysical techniques in permeability prediction. Limestone is the predominant lithology of the formation, as confirmed by the Density-Neutron cross-plot investigation. It is a suitable reservoir because of its low shale volume, specifically MB21, MC1, and MC2, which indicate a clean carbonate reservoir. MB21 is the principal pay zone, a poorly water-saturated, highly porous, and permeable zone. While MC1 is moderately water-saturated and porous, MC2 is not a favorable productive zone because it is close to the oil-water contact and has higher water saturation. The classical permeability prediction method exhibited high dispersion due to formation heterogeneity. To deal with this issue, the HFU method was combined with the Bootstrap Forest to improve permeability prediction. This combination proves the success of this workflow in dealing with the reservoir complexity and reducing prediction uncertainty. The detailed petrophysical assessment of the Mishrif Formation can improve reservoir management and production optimization, further enhancing decision-making in future field development plans.

## NOMENCLATURE

Symbol	Description	Symbol	Description
<b>a</b>	Lithology constant, dimensionless	<b>R<sub>w</sub></b>	Formation water resistivity, $\Omega \cdot m$
<b>FZI</b>	Flow Zone Indicator, $\mu m$	<b>S<sub>w</sub></b>	Water Saturation, fraction
<b>GR<sub>log</sub></b>	Gamma ray reading of formation, API	<b>V<sub>sh</sub></b>	Shale Volume, fraction
<b>GR<sub>max</sub></b>	The maximum gamma ray, API	<b><math>\phi_D</math></b>	density porosity, fraction
<b>GR<sub>min</sub></b>	The minimum gamma ray, API	<b><math>\phi_{ND}</math></b>	Neutron-density porosity, fraction
<b>I<sub>GR</sub></b>	Gamma-ray index	<b><math>\phi_s</math></b>	Sonic porosity, fraction
<b>K</b>	Permeability, md	<b><math>\phi_{sh}</math></b>	Shale porosity, fraction
<b>m</b>	Cementation exponent, dimensionless	<b><math>\phi_z</math></b>	Normalized porosity, fraction
<b>n</b>	Saturation exponent, dimensionless	<b><math>\Delta t_f</math></b>	Transit time in formation fluid, $\mu sec/ft$
<b>PHIE</b>	effective porosity, fraction	<b><math>\Delta t_{log}</math></b>	Transit time in the matrix, $\mu sec/ft$
<b>POR</b>	total porosity, fraction	<b><math>\rho_b</math></b>	Bulk density, gm/cc
<b>RQI</b>	reservoir quality index, $\mu m$	<b><math>\rho_f</math></b>	Fluid density, gm/cc
<b>RT</b>	formation resistivity, $\Omega \cdot m$	<b><math>\rho_{ma}</math></b>	Matrix density, gm/cc

## Acknowledgements

The authors thank the Department of Petroleum Engineering, University of Baghdad for their valuable support and constructive feedback that improved this work.

## Credit Authorship Contribution Statement

Layth Hameed Abd Ali: Writing – review and editing, Writing – original draft, Software, Methodology. Sameera Mohamed Hamd-Allah: review, Validation.

## Declaration of Competing Interests

The authors declare that they have no known competing financial interests or personal relationships that could have appeared to influence the work reported in this paper.



## REFERENCES

- Abdulelah, H., Mahmood, S., and Hamada, G., 2018. Hydraulic flow units for reservoir characterization: A successful application on arab-d carbonate. *IOP Conference Series: Materials Science and Engineering*. IOP Publishing, P. 012020. <https://doi.org/10.1088/1757-899X/380/1/012020>
- Abnavi, A.D., Karimian Torghabeh, A., and Qajar, J., 2021. Hydraulic flow units and ANFIS methods to predict permeability in heterogeneous carbonate reservoir: Middle East gas reservoir. *Arabian Journal of Geosciences*, 14, pp. 1-10. <https://doi.org/10.1007/s12517-021-07084-5>
- Abd Ali, L.H., and Hamd-Allah, S. M., 2026. Permeability estimation using the HFU method enhanced by bootstrap forest AI-approach for FZI prediction in the Mishrif Reservoir, Southern Iraq. *Iraqi National Journal of Earth Science (INJES)*, 26
- Ahmed, K. H., 2022. Improving sweep efficiency of water flooding for Mishrif Formation- Buzurgan Oil Field. PhD thesis, Department of Petroleum Engineering, University of Baghdad, Iraq.
- Al-Dujaili, A. N., 2023. Reservoir rock typing and storage capacity of Mishrif Carbonate Formation in West Qurna/1 Oil Field, Iraq. *Carbonates Evaporites*, 38, P. 83. <https://doi.org/10.1007/s13146-023-00908-3>
- Al-Dujaili, A. N., Shabani, M. and Al-Jawad, M. S., 2021. Identification of the best correlations of permeability anisotropy for Mishrif reservoir in West Qurna/1 oil Field, Southern Iraq. *Egyptian Journal of Petroleum*, 30, pp. 27-33. <https://doi.org/10.1016/j.ejpe.2021.06.001>
- Al-Dujaili, A. N., Shabani, M. and Al-Jawad, M. S., 2023. Effect of heterogeneity on capillary pressure and relative permeability curves in carbonate reservoirs. A case study for the Mishrif formation in West Qurna/1 Oilfield, Iraq. *Iraqi Journal of Chemical Petroleum Engineering*, 24, pp. 13-26. <https://doi.org/10.31699/IJCPE.2023.1.3>
- Al-Ameri, N. J. and Hamd-Allah, S. M., 2023. Sonic scanner helps in identifying reservoir potential and isotropic characteristics of Khasib Formation. *The Iraqi Geological Journal*, 129-143. <https://doi.org/10.46717/igj.56.1D.11ms-2023-4-20>
- Al Hussein, A. K. and Hamd-Allah, S. M., 2024. Prediction of petrophysical properties using neural network technique for Mishrif reservoir-Southern of Iraq. AIP Conf. Proc. 3090, 020004. <https://doi.org/10.1063/5.0227959>
- Al Jawad, M. S. and Tariq, B. Z., 2019. Estimation of cutoff values by using regression lines method in Mishrif reservoir/Missan oil fields. *Journal of Engineering*, 25(2), pp. 82-95. <https://doi.org/10.31026/j.eng.2019.02.06>
- Aldarraji, M. Q. and Almayahi, A. Z., 2019. Seismic structure study of Buzurgan Oil field, Southern Iraq. *Iraqi Journal of Science*, pp. 610-623. <https://ijs.uobaghdad.edu.iq/index.php/eijs/article/view/703>
- Alhusseini, A. K. and Hamd-Allah, S., 2022. Estimation of initial oil in place for Buzurgan Oil Field by using volumetric method and reservoir simulation method. *The Iraqi Geological Journal*, pp. 108-122. <https://doi.org/10.46717/igj.55.2C.9ms-2022-08-22>
- Alobaidi, D. A., 2016. Permeability prediction in one of Iraqi carbonate reservoir using hydraulic flow units and neural networks. *Iraqi Journal of Chemical and Petroleum Engineering*, 17 (1), pp. 1-11. <https://doi.org/10.31699/IJCPE.2016.1.1>



- Amaefule, J. O., Altunbay, M., Tiab, D., Kersey, D. G. and Keelan, D. K., 1993. Enhanced reservoir description: using core and log data to identify hydraulic (flow) units and predict permeability in uncored intervals/wells. SPE Annual Technical Conference and Exhibition. SPE, SPE-26436-MS. <https://doi.org/10.2118/26436-MS>
- Anifowose, F. A., Abdurraheem, A., Al-Shuhail, A. and Schmitt, D. P., 2013. Improved permeability prediction from seismic and log data using artificial intelligence techniques. *SPE middle east oil and gas show and conference*. SPE, SPE-164465-MS. <https://doi.org/10.2118/164465-MS>
- Astsaouri, T., Habiburrahman, M., Ibrahim, A. F. and Wang, Y., 2024. Utilizing machine learning for flow zone indicators prediction and hydraulic flow unit classification. *Scientific Reports*, 14, 4223. <https://doi.org/10.1038/s41598-024-54893-1>
- Bassiouni, Z., 1994. Theory, measurement, and interpretation of well logs. Society of Petroleum Engineers. <https://doi.org/10.2118/9781555630560>
- Bateman, R. M., 2012. Formation Evaluation Overview. *Openhole Log Analysis and Formation Evaluation*. Society of Petroleum Engineers (SPE).
- Borhani, T.N.G. and Emadi, S.H., 2011. Application of hydraulic flow units and intelligent systems for permeability prediction in a Carbonate Reservoir. In *CUTSE International Conference*. <http://dx.doi.org/10.13140/RG.2.2.23338.72648>
- Bouffin, N. and Jensen, J. L., 2009. Efficient detection of productive intervals in oil and gas reservoirs. *PETSOC Canadian International Petroleum Conference*. PETSOC, PETSOC-2009-125. <https://doi.org/10.2118/2009-125>
- Causey, G. L., 1991. *Computer determination and comparison of volume of clay derived from petrophysical and laboratory analysis*. Texas Tech University. <http://hdl.handle.net/2346/15744>
- Dewan, J.T., 1983. Essentials of modern open-hole log interpretation: PennWell Publ. Co., Tulsa Oklahoma, p.361.
- Egbele, E., Ezuka, I. and Onyekonwu, M., 2005. Net-To-Gross Ratios: Implications in Integrated Reservoir management studies. Nigeria annual international conference and exhibition. SPE-98808-MS. <https://doi.org/10.2118/98808-MS>
- Hamd-Allah, S. M., Noor, B. M. and Watten, A. R., 2016. Permeability prediction for Nahr-Umr reservoir/Subba field by using FZI method. *Journal of Engineering*, 22(9), pp. 160-171. <https://doi.org/10.31026/j.eng.2016.09.10>
- Horsfall, O., Uko, E. and Tamunobereton-Ari, 2013. Comparative analysis of sonic and neutron-density logs for porosity determination in the South-eastern Niger Delta Basin, Nigeria. *American Journal of Scientific Industrial Research*, 4, pp. 261-271. <https://doi.org/10.5251/ajsir.2013.4.3.261.271>
- Khashman, M. A., Shirazi, H., and Al-Dujaili, A. N., 2025. Comparative evaluation of productivity indicators in carbonate reservoir modeling by a case study for the Mishrif Formation in the Iraqi Buzurgan Oilfield. *Discover Geoscience*, 3(17). <https://doi.org/10.1007/s44288-025-00118-5>
- Mohammadian, E., Kheirollahi, M., Liu, B., Ostadhassan, M. and Sabet, M., 2022. A case study of petrophysical rock typing and permeability prediction using machine learning in a heterogeneous carbonate reservoir in Iran. *Scientific Reports*, 12, P. 4505. <https://doi.org/10.1038/s41598-022-08575-5>





- Mohammed, M.M. and Salih, H.M., 2025. Permeability Determination of The Mishrif Carbonate Reservoir in Buzurgan Oilfield Using the Integration Between Well Logs and Regression Analysis Technique. *Iraqi National Journal of Earth Science (INJES)*, 25(1), pp. 17-29. <https://doi.org/10.33899/earth.2023.143801.1156>
- Pickett, G., 1966. A review of current techniques for determination of water saturation from logs. *Journal of Petroleum Technology*, 18, pp. 1425-1433. <https://doi.org/10.2118/1446-PA>
- Rider, M. H., 2002. *The Geological Interpretation of Well Logs*, Rider-French Consulting.
- Schön, J. H., 2011. *Physical properties of rocks: A workbook*, Elsevier.
- Sebtosheikh, M. A., Motafakkerfard, R., Riahi, M.-A., Moradi, S. and Sabety, N., 2015. Support vector machine method, a new technique for lithology prediction in an Iranian heterogeneous carbonate reservoir using petrophysical well logs. *Springer Nature*, 30, pp. 59-68. <https://doi.org/10.1007/s13146-014-0199-0>
- Shah, M. S., Khan, M. H. R., Rahman, A., Islam, M. R., Ahmed, S. I., Molla, M. I. and BuTT, S., 2021. Petrophysical evaluation of well log data for reservoir characterization in Titas gas field, Bangladesh: A case study. *Journal of Natural Gas Science Engineering*, 95, P. 104129. <https://doi.org/10.1016/j.jngse.2021.104129>
- Skrettingland, K., Holt, T., Tweheyo, M. T. and Skjevrak, I., 2011. Snorre low-salinity-water injection—coreflooding experiments and single-well field pilot. *SPE Reservoir Evaluation & Engineering*, 14, pp. 182-192
- Stephens, D. B., Hsu, K.C., Prieksat, M. A., Ankeny, M. D., Blandford, N., Roth, T. L., Kelsey, J. A., and Whitworth, J. R., 1998. A comparison of estimated and calculated effective porosity. *Hydrogeology Journal*, 6, pp. 156-165. <https://doi.org/10.1007/s100400050141>
- Tiab, D., and Donaldson, E. C., 2012. Petrophysics: theory and practice of measuring reservoir rock and fluid transport properties. *Elsevier/Gulf Professional Pub.*,
- Worthington, P. F., 1993. The uses and abuses of the Archie equations, 1: The formation factor-porosity relationship. *Journal of Applied Geophysics*, 30, pp. 215-228. [https://doi.org/10.1016/0926-9851\(93\)90028-W](https://doi.org/10.1016/0926-9851(93)90028-W)
- Zelenika, K. N., Vidaček, R., Ilijaš, T. and Pavić, P., 2017. Application of the deterministical and stochastic geostatistical methods in petrophysical modelling—a case study of Upper Pannonian reservoir in Sava Depression. *Geologia Croatica*, 70, pp. 105-114. <https://doi.org/10.4154/gc.2017.10>
- Zhang, X., Li, D., Zhang, M. and Li, C., 2018, July. Logging evaluation of permeability in Heterogeneous conglomerate reservoir. In *Proceedings of the International Field Exploration and Development Conference 2017*, pp. 155-164. Singapore. [https://doi.org/10.1007/978-981-10-7560-5\\_14](https://doi.org/10.1007/978-981-10-7560-5_14)

## تقييم الخصائص البتروفيزيائية لمكمن المشرف في جنوب العراق عبر الذكاء الاصطناعي لتعزيز حساب النفاذية

ليث حميد عبد علي\*، سميرة محمد حمد الله

قسم هندسة النفط، كلية الهندسة، جامعة بغداد، بغداد، العراق

### الخلاصة

يُعَدُّ التفسير الدقيق للخصائص البتروفيزيائية عاملاً أساسياً في تحسين عمليات استكشاف الهيدروكربونات والتخطيط لعمليات للإنتاج. تهدف هذه الدراسة إلى إجراء تحليل بتروفيزيائي شامل لتكوين المشرف في حقل بزركان النفطي، وذلك من خلال استعمال كل من أساليب التفسير البتروفيزيائي التقليدية مع تقنيات الذكاء الاصطناعي (AI) تم استخدام سجلات الآبار، بما في ذلك  $\gamma$  ray، density، neutron، sonic، resistivity جنباً إلى جنب مع قياسات اللباب الصخري، لتحديد خصائص المكمن، مثل التكوين الصخري، حجم shall، والمسامية، والنفاذية، وتشبع المياه، وبالتالي يمكن تقدير نسبة العمق المنتج. أظهرت طرق التقليدية للتنبؤ بالنفاذية، لا سيما العلاقات بين نفاذية اللباب ومسامية تشتتاً كبيراً بسبب الطبيعة غير المتجانسة للمكمن. للحصول على دقة أعلى في التنبؤ بنفاذية الصخور، تم دمج كل من طريقة الوحدات الهيدروليكية (HFU) مع نموذج الذكاء الاصطناعي Bootstrap Forest، مما أدى إلى تحسين دقة تقدير النفاذية بشكل واضح. أوضحت النتائج أن طبقة MB21 هي منطقة الإنتاج الرئيسية، حيث تتميز بتشبع هيدروكربوني مرتفع ومسامية عالية. يعد استعمال كل من تقنيات البتروفيزيائي ونموذج التنبؤ بالنفاذية القائم على الذكاء الاصطناعي أساساً قوياً لتوصف المكامن. تؤكد هذه النتائج على الدور الفعال للأساليب الحسابية المتقدمة في تقييم الطبقات تحت سطح الأرض، مما يساعد على تقليل عدم الدقة في النتائج المرتبطة بالمكامن المعقدة.

**الكلمات المفتاحية:** خصائص المكامن، تقنيات الذكاء الصناعي، طريقة بوتستراب فورست، طريقة الوحدات الهيدروليكية، حقل بزركان النفطي.